Proceedings of the 3rd International Conference on Green Energy, Environment and Sustainable Development (GEESD2022), X. Zhang et al. (Eds.)

doi:10.3233/ATDE220345

Ammonia Inhibition Effects on Performance of a Continuous Stirred Bioelectrochemical System

Haiman WANG[1], Yeting ZHANG and Guiqiang WANG
School of Municipal and Environmental Engineering, Shenyang Jianzhu University. Shenyang 110168, Liaoning, China

Abstract. Continuous stirred bioelectrochemical system (CSBES), consisting of anaerobic digestion reaction zone (ADRZ) and bioelectrochemical reaction zone (BERZ), was constructed to investigate the ammonia inhibitory effects on the performance of electricity generation and wastewater treatment. Continuous experiments were conducted with ammonia concentration ranging from 300 mg/L to 1200 mg/L. As the ammonia concentration increasing from 300 mg/L to 900 mg/L, both of the maximum power densities and the COD removal increased. When the ammonia concentration reached to 1200 mg/L, the maximum power densities of the four cells decreased by 55.7%, 58.9%, 58.0% and 60.6% in comparison with that under ammonia concentration of 900 mg/L. The COD removal reduced to 71.2 ± 1.4%, leading to COD concentration in the effluent increased to 1758 ± 93 mg/L. Electrochemical measurements revealed that the deterioration of anode performance caused the reduction of power generation. The conductivity control experiment showed that the toxic effects of high ammonia concentration on exoelectrogens caused performance deterioration of the CSBES. The threshold ammonia concentration that triggered the inhibition effect on exoelectrogens in CSBES was 1200 mg/L, and the anaerobic consortium in ADRZ could tolerant to higher ammonia concentration than the exoelectrogens in BERZ.

Keywords. Continuous stirred bioelectrochemical system, ammonia inhibition, electricity generation, wastewater treatment

1. Introduction

Bioelectrochemical system (BES) is an environmentally friendly device that can effectively convert organics into electrical energy using electrochemically active bacteria as catalyst [1]. BES is expected to be applied in wastewater treatment and renewable energy recovery [2, 3], and has outstanding properties such as pollution free, high energy invert efficiency and wide scope of application. Various types of wastewater have been used as feed in BES, such as swine wastewater [4], human urine [5], fermented wastewater [6], etc. However, some BESs do not perform well in high-strength wastewater because of physical, chemical and biological restrictions, which reduce the activity of exoelectrogenic bacteria and inhibit electron transfer to the anode [7]. To meet the requirement of dealing with high-strength wastewater with

[1] Corresponding Author, Haiman WANG, School of Municipal and Environmental Engineering, Shenyang Jianzhu University, Shenyang 110168, Liaoning, China; Email: 12b327018@hit.edu.cn.

refractory organics, BESs with different configurations have been constructed, among which AD (anaerobic digestion)-BES integrated system is an effective configuration. Many of the limitations of BES can be alleviated due to the complementary synergy between AD and BES. This novel coupled system has been shown to improve tolerance to high-strength organics, enhance pollutant removal and energy recovery from wastewater [8].

Ammonia nitrogen is a common pollutant in wastewater and is important to maintain the stability of anaerobic digestion. However, high ammonia can affect the performance of AD processes because it directly inhibits microbial activity [9]. In addition to being present in the liquid to be digested, ammonia also accumulates during breakdown of the nitrogenous matter [10]. Recent studies have found that due to its high permeability to cell membranes, free ammonia is considered to be the primary reason for inhibition of methanogenic consortium in nitrification tanks [11], and its equilibrium concentration depends on pH and temperature [12]. Mechanisms of ammonia inhibition include destruction of enzyme activity, pH change inside the cell and cell dehydration because of high osmotic pressure [11, 13, 14]. Many methods to alleviate ammonia inhibition in AD have been reported recently, such as bioaugmentation [15, 16], struvite precipitation [17], supplementation of certain trace element [18, 19], adjustment of C:N ratio [20], supplementation of via nano-bubble water [21] and supplementation of magnetite and polyurethane foam carrier [22].

Excessive amounts of ammonia in the wastewater also have negative effects on the exoelectrogens in BES, and thus reduce its electrical performance and removal efficiency of organic pollutants [7, 23-25]. Due to the influence of various operational factors, the threshold ammonia concentration triggering the inhibitory effects in BESs is not the same according to the previous studies [26]. It is reported that ammonia concentration of 500 mg-NL^{-1} can cause limitation on bioanode in a single-chambered BES [7]. However, no cytotoxic effects of ammonia were observed at concentration up to 4000 mg-NL^{-1} in a two chamber BES [27]. To promote BES treating ammonia-rich wastewater, a two-chamber BES consisting of nitrifying granular sludge was developed, and achieved a high ammonia removal efficiency of 98.55% at ammonia concentration of 200 mg-NL^{-1} [28]. A heterotrophic nitrifying/denitrifying air-cathode BES was operated with ammonia-polluted wastewater, which removed 99% of ammonia and 95% of total nitrogen [29]. Although the ammonia inhibitor effects in AD and BES have been respectively studied, there are relatively few research on ammonia inhibition in AD-BES integrated system. However, it is crucial to study these effects on syntrophic reaction when these two processes are integrated.

In this study, a continuous stirred bioelectrochemical system (CSBES) constructed by combing AD and BES, was operated to study the ammonia inhibition on the performance of electricity generation and wastewater treatment. Control experiments on conductivity were conducted to evaluate the net inhibition effect of ammonia. The effluent quality from different functional zones of CSBES were measured to determine the inhibition intensity of ammonia on anaerobic consortium and exoelectrogens.

2. Materials and Methods

2.1. CSBES Configuration

The continuous stirred bioelectrochemical system (CSBES) was developed by combing anaerobic digestion and bioelectrochemical system (Figure 1a) [30]. It was composed of an anaerobic digestion reaction zone (ADRZ) and a bioelectrochemical reaction zone (BERZ) (Figures 1b and 1c). The cylindrical ADRZ was inoculated with anaerobic activated sludge, and the mixed liquid suspended solids were continuously mixed by a micro-motor. The rectangular BERZ was divided into four separate cells, with each cell using carbon fiber brush as anode [31] and rolling-pressed activated carbon as cathode [32]. A three-phase separator was installed between the ADRZ and BERZ, which was also playing a role as solid-liquid-gas separator and gas collector.

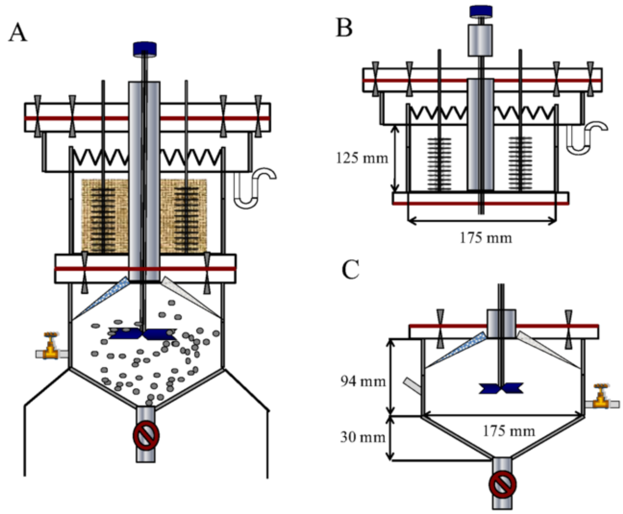

Figure 1. (a) The continuous stirred bioelectrochemical system (CSBES); (b) Bioelectrochemical reaction zone (BERZ); (c) anaerobic digestion reaction zone (ADRZ).

2.2. Operation Procedures

The CSBES feeding with sucrose wastewater had been run for four months before this research. In this experiment, artificial wastewater was employed as the influent, which included: sucrose 5.3 g/L; phosphate buffer solution without NH_4Cl 50mmol/L; vitamin mixture 1mL/L and trace metal 1mL/L [33]. To investigate how ammonia influences power production and wastewater treatment in CSBES, tests were conducted in four phases by increasing ammonia content in the artificial wastewater gradually. The ammonia concentration was increased from 300 mg/L to 1200 mg/L in a stepwise manner by gradually increasing the contents of NH_4Cl (1.14 g/L to 4.59 g/L) in the artificial wastewater. The system was run for 15 days at every ammonia concentration to achieve stable performance. The hydraulic retention time of the system was 12 h and each cell was connected to an external resistor of 10 Ω. In each phase, performance of power generation and wastewater treatment was assessed.

To exclude the influence of conductivity, a control experiment was conducted to determine the net impact of ammonia on the CSBES performance. As a conductivity control, the conductivity of the synthetic wastewater was adjusted by KCl (KCl-CSBES), and the KCl-CSBES was operated in the same condition as the NH_4Cl-CSBES.

2.3. Analytical Methods

The voltage outputs of the CSBES were taken at 30 min intervals throughout the experiments via a data acquisition system (PISO-813). As the performance of the CSBES stabilized, polarization curves were conducted to calculate the maximum power density. The polarization curves were performed on a workstation in a potential range from open-circuit voltage to zero. Cyclic voltammetry (CV) measurements were performed in the potential range from minus 0.8 V to 0.2 V with carbon fiber brush anode as the working electrode. Both of the polarization curves and CV were performed at a scan rate of 1 mV/s. Power density (normalized by the cathode area) was calculated as previously described [34]. Measurements of COD, ammonia, nitrite and nitrate were conducted based on the Standard Methods (APHA 1998).

3. Results and Discussion

3.1. Effects of Ammonia Concentration on Electricity Generation of CSBES

Under the condition that the influent organic loading rate was maintained at 12 kg COD/m^3/d, different ammonia concentrations (300,600,900 and 1200 mg/L) were obtained by gradually increasing the contents of NH_4Cl (1.14 g/L, 2.29 g/L, 3.44 g/L and 4.59 g/L) in the synthetic wastewater. Electricity generation performance of CSBES was investigated under each condition. The system was run for at least 15 days at each ammonia concentration to ensure stable performance.

The average current densities of these four cells increased from 3.54 A/m^2 ± 0.01 A/m^2 to 4.43 A/m^2 ± 0.03 A/m^2 after elevating the ammonia concentration from 300 mg/L to 900 mg/L (Figure 2.), presenting a gradual upward trend. The increase in current density might be due to the increased conductivity of the feed, which increased by 55.2% from 8.46 mS/cm to 13.13 mS/cm as the ammonia concentration increased from 300 mg/L to 900 mg/L. The increase in conductivity can accelerate the transfer rate of ions or protons in the solution to the cathodic three-phase interface reaction zone, thus decreasing the ohmic internal resistance and increasing its current density [35]. As the ammonia concentration increased to 1200 mg/L, the influent conductivity increased to 15.49 mS/cm, resulting in a gradual decline trend of the average current densities of the system. After about 27 days of operation, the mean current densities eventually decreased from 4.19 A/m^2 ± 0.07 A/m^2 to 0.48 A/m^2 ± 0.21 A/m^2 (Figure 2).

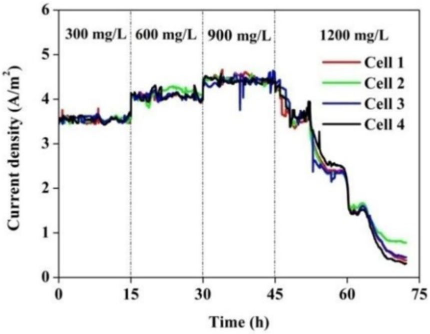

Figure 2. Current generation of CSBES at different ammonia concentrations.

Polarization curves of CSBES (Figure 3) were plotted as gradually increasing ammonia concentrations. The maximum power densities of these four cells increased as the ammonia concentration increased from 300 mg/L to 900 mg/L due to the increase in influent conductivity. When the ammonia concentration was 900 mg/L, the maximum power densities of the four cells were 663 mW/m^2, 701 mW/m^2, 647 mW/m^2 and 689 mW/m^2, which were enhanced by 13.5%, 26.3%, 17.2% and 20.5% respectively compared with that under ammonia concentration of 300 mg/L. The maximum power densities of the four cells drastically decreased when the ammonia concentration increased to 1200 mg/L, which were decreased by 55.7%, 58.9%, 58.0% and 60.6%. Polarization curves revealed that the open circuit voltages of the four cells were significantly different when the ammonia nitrogen concentration was 900 mg/L and 1200 mg/L. The open circuit voltages of the four cells were 612, 601, 605 and 613 mV (Figure 3c) at 900 mg/L, which decreased to 440,423,420 and 420 mV when ammonia concentration increased to 1200 mg/L, and the maximum circuit current of the four cells dropped to 2.4 A/m^2, 2.3 A/m^2, 2.0 A/m^2 and 2.4 A/m^2 (Figure 3d).

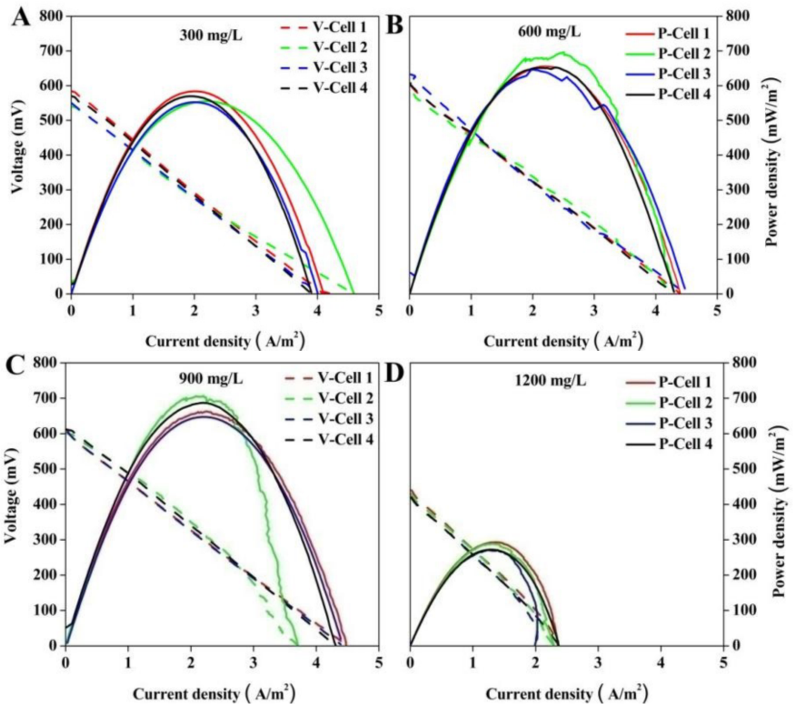

Figure 3. Polarization curves and power densities of the CSBES at different ammonia concentrations. (a): 300 mg/L; (b): 600 mg/L; (c): 900 mg/L; (d): 1200 mg/L.

Electrode polarization curves were used to determine the main reasons affecting the difference in electricity generation performance of the four cells. It showed that the cathode potential had no significant change when the ammonia concentration increased from 900 mg/L to 1200 mg/L, and the average open circuit potential of the four cathode was 147 mV ± 5 mV and 140 mV ± 3 mV (Figure 4). However, the average open circuit potential of the anode increased by 37.9% ± 2.3% from -464 mV ± 4 mV to -288 mV ± 12 mV as ammonia concentration increased from 900 mg/L to 1200 mg/L. From the perspective of maximizing the energy output of the bioelectrochemical system, a more negative anode potential is better for power generation. Thus, it can be determined that the decrease of anode performance caused the decrease of current density and maximum power density at ammonia concentration of 1200 mg/L. The high osmotic pressure caused by the high conductivity (15.49 mS/cm), or the toxic effect of high ammonia concentration (1200 mg/L) on exoelectrogens, might be the reasons for the decline of anode performance.

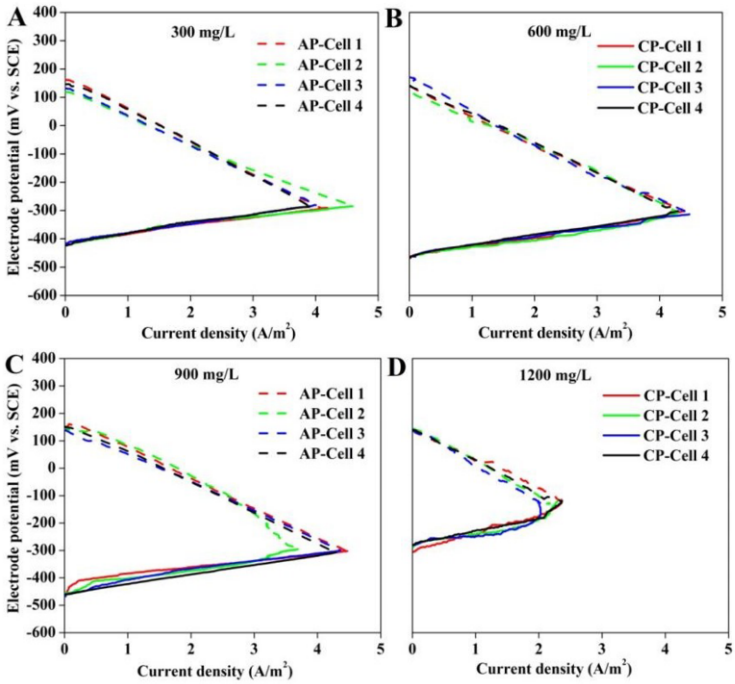

Figure 4. Electrode potentials of the CSBES at different ammonia concentrations. (a): 300 mg/L; (b): 600 mg/L; (c): 900 mg/L; (d): 1200 mg/L.

3.2. Effect of Ammonia Concentration on Wastewater Treatment of CSBES

Effluent COD of the system was measured at each phase to investigate the influence of ammonia concentration on wastewater treatment efficiency. As the ammonia concentration increased from 300 mg/L to 900 mg/L, COD removal of the system increased from 87.3% ± 1.1% to 90.9% ± 0.8%, and the COD concentration in the effluent decreased from 776 mg/L ± 47 mg/L to 553 mg/L ± 56 mg/L (Figure 5). The increase of current density might cause the increase in COD removal. The degradation rate of organic matter by exoelectrogens was accelerated under high current density, thus the COD removal was enhanced due to the improved performance of the bioelectrochemical reaction zone (BERZ).

However, COD removal of the system decreased to 71.2% ± 1.4% when ammonia concentration reached to 1200 mg/L, resulting in an increase of the COD concentration in the effluent to 1758 mg/L ± 93 mg/L. The ammonia inhibition on the activity of exoelectrogens in the BERZ, or the inhibition on anaerobic consortium in the anaerobic digestion reaction zone (ADRZ), might be the reasons for the decline of the COD removal performance. In addition, the disrupted syntrophic effect between bioelectrochemical reactions and anaerobic digestion, which was probably caused by the ammonia inhibition on one of these two functional microbial consortium, might also cause the decrease in the COD removal.

In the process of gradually increasing ammonia concentration of the influent, the ammonia removal performance was also investigated. However, by monitoring the concentrations of NH_4^+-N, NO_3^--N and NO_2^--N in the effluent, it was observed that ammonium could not be removed in CSBES. In each stage of gradually increasing the ammonia concentration, the effluent ammonia concentration was basically the same as that in the influent, and the ammonia removal fluctuated in the range of 9.8 to 15.5%. In addition, NO_3^--N and NO_2^--N was rarely detected in the effluent. The possible reason for the poor effect of CSBES on ammonia removal was that the nitrification in the system was weak or there was no nitrification process, and ammonia removal in the CSBES was possibly accomplished by sludge adsorption or microorganisms assimilation.

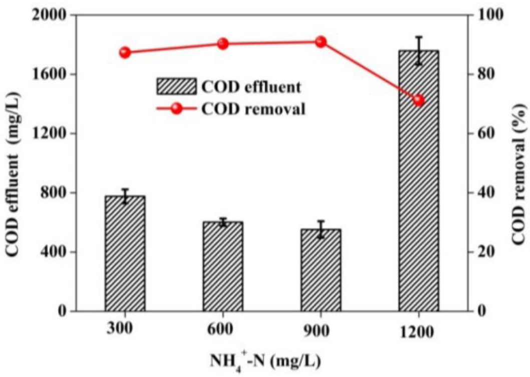

Figure 5. Effluent COD and COD removal in CSBES at different ammonia concentrations.

3.3. Mechanism of ammonia inhibition on the performance of CSBES

To further explore the ammonia inhibition mechanism on CSBES performance, effluent quality of the ADRZ and BERZ was detected to determine the inhibition intensity of ammonia on these two functional zones. COD removal of the ADRZ slightly reduced from 62.2% ± 2.1% to 55.8% ± 3.7% as the ammonia concentration increasing from 900 mg/L to 1200 mg/L, resulting the COD concentration increased from 2287 mg/L ± 97 mg/L to 2709 mg/L ± 159 mg/L in the effluent (Figure 6). However, the effluent COD concentration increased significantly from 552 mg/L ± 55 mg/L to 1758 mg/L ± 93 mg/L as the ammonia concentration increasing from 900 to 1200 mg/L, resulting in a decrease of the COD removal by 53.7%. Effluent quality monitoring results showed the inhibitory effects of high ammonia on the BERZ was more intensive than that on the ADRZ.

In order to prevent the system performance from deteriorating, ammonia concentration in the influent was reduced from 1200 mg/L to 900 mg/L when the output voltage of the four cells was dropped to about 30 mV, so as to improve the operation status of the system and restore its performance to the levels at ammonia concentration of 900 mg/L. During 30 days operation, the COD and volatile acid concentrations in the effluent continued to decrease and the current density of the four cells gradually increased, and the mean current density finally reached to 4.31 A/m^2 ± 0.05 A/m^2, indicating that the system performance had basically recovered to the original level.

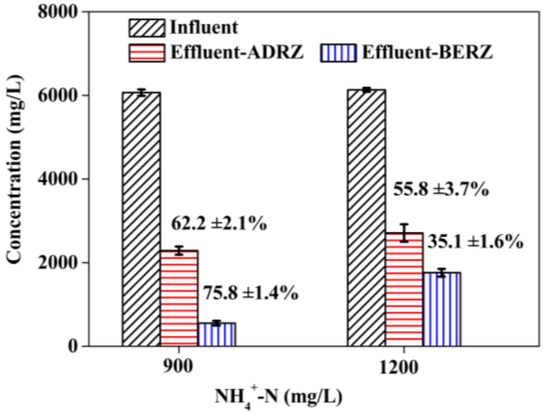

Figure 6. Effluent COD of ADRZ and BERZ at ammonia concentration of 900 mg/L and 1200 mg/L.

In order to determine whether the deterioration of performance was caused by high conductivity or the toxic effect of high ammonia concentration, a conductivity control experiment was conducted by replacing NH_4Cl with KCl, and the influent conductivity was the same as that at ammonia concentration of 1200 mg/L (15.49 mS/cm). The maximum power densities of the four cells under the condition of KCl were 653 mW/m^2 ± 10 mW/m^2, 698 mW/m^2 ± 9 mW/m^2, 622 mW/m^2 ± 5 mW/m^2 and 653 mW/m^2 ± 13 mW/m^2, which were nearly unchanged compared with that under ammonia concentration of 900 mg/L, indicating that the maximum power densities of the system were not inhibited in the process of increasing the influent conductivity from 13.13 mS/cm to 15.49 mS/cm (Figure 7). However, the maximum power densities of the four cells increased by 117.3% ± 4.7%, 138.1% ± 3.3%, 149.3% ± 11.2% and 135.9% ± 3.1% compared with that under ammonia concentration of 1200 mg/L, further indicating that the increase of conductivity was not the reason for the reduction of the maximum power densities of the system. The polarization curves indicated that the discrepancy in anode potential caused the difference of the maximum power densities of the system at the ammonia concentration of 1200 mg/L and KCl.

The change trend of the maximum power densities of the four cells in the system under the three conditions was consistent, indicating that the changes in the conductivity and composition of the influent had the same effect on each cell. Taking cell 1 as an example, CV was employed to evaluate the effects of three influent conditions on the exoelectrogens activity. Under the ammonia concentration of 900 mg/L and KCl, the maximum anodic current was basically the same (34.5 mA and 33.7 mA) (Figure 8), which was consistent with the results of the anode polarization curve, indicating that there was no difference in the activity of exoelectrogens under the two conditions. The maximum current of the anode dropped significantly to 11.3 mA at ammonia concentration of 1200 mg/L, indicating that the electrocatalytic activity was weakened and the exoelectrogens were obviously inhibited by high ammonia concentration.

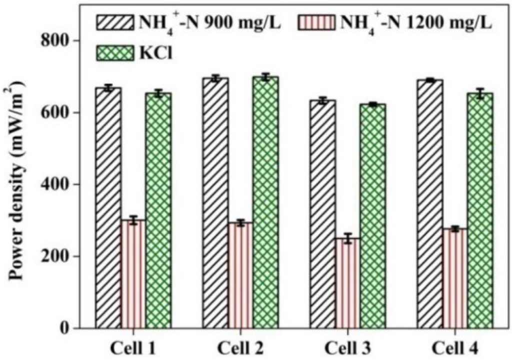

Figure 7. The maximum power densities of CSBES under NH_4Cl and KCl conditions.

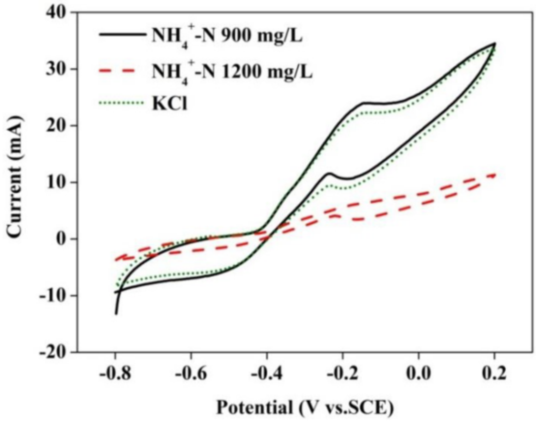

Figure 8. Cyclic voltammogram of anode biofilm (Cell 1) under NH_4Cl and KCl conditions.

Results showed that the threshold ammonia concentration that triggered the inhibition effect on exoelectrogens in CSBES was 1200 mg/L. In addition, the anaerobic consortium in ADRZ could tolerate to high ammonia concentration better than the exoelectrogens in BERZ. Two theories of ammonia inhibition are proposed (1) unionized ammonia deteriorate the activity of cytosolic enzymes directly; (2) hydrophobic ammonia molecular is quickly changed to ammonium because of intracellular pH after it passively diffuses into the bacterial cells. The accumulation of ammonium can lead to inhibition of cell activity by changing pH inside a cell. Previous research was different regarding the threshold ammonia concentration that triggered the inhibition effect on exoelectrogens. Nam found that the current output of a single-chambered BES operating under batch mode was significantly reduced when the concentration of TAN exceeded 500mg-N/L. Meanwhile, the maximum power density of the system decreased from 4240 mW/m³ to 1700 mW/m³ when TAN concentration increasing from 500 mg-N/L to 4000 mg-N/L [7]. In a continuous single-chamber BES, the maximum power density was still not inhibited as TAN concentrations increased to 3500 mg-N/L [23]. It is reported that the threshold ammonia concentration that triggered the inhibition effect on exoelectrogens is influenced by many reasons, such as the operation method, pH of influent, substrate concentration and operating temperature [26]. In addition, a proper period of microbial acclimation can make the activity of exoelectrogens more tolerant to high ammonia concentration.

4. Conclusion

A high ammonia concentration of 1200 mg/L for an AD-BES integrated system could cause inhibitory effects on power generation, and consequently reduce the COD removal efficiency. The toxic effect of high ammonia concentration on the exoelectrogens was the main reason that caused the performance deterioration of the system. The anaerobic consortium in ADRZ was more tolerant of high ammonia concentration than the exoelectrogens in BERZ. The work could provide a reference for the study of ammonia inhibitory effects in AD-BES integrated system.

Acknowledgments

This work was supported by the National Natural Science Foundation of China (Grant No. 51908377), China Postdoctoral Science Foundation (Grant No. 2018M641713).

References

[1] Oh SE, Logan BE. Proton exchange membrane and electrode surface areas as factors that affect power generation in microbial fuel cells. Applied Microbiology and Biotechnology. 2006;70(2):162-9.
[2] Park Y, Park S, Nguyen VK, Yu J, Torres CI, Rittmann BE, et al. Complete nitrogen removal by simultaneous nitrification and denitrification in flat-panel air-cathode microbial fuel cells treating domestic wastewater. Chemical Engineering Journal. 2017;316(3):117-29.
[3] Wu D, Sun F, Chua FJD, Zhou Y. Enhanced power generation in microbial fuel cell by an agonist of electroactive biofilm—Sulfamethoxazole. Chemical Engineering Journal. 2020;384:123238.
[4] Kim JR, Dec J, Bruns MA, Logan BE. Removal of odors from Swine wastewater by using microbial fuel cells. Applied and Environmental Microbiology. 2008;74(8):2540-3.
[5] Kuntke P, Śmiech KM, Bruning H, Zeeman G, Saakes M, Sleutels THJA, et al. Ammonium recovery and energy production from urine by a microbial fuel cell. Water Research. 2012;46(8):2627-36.
[6] Christou ML, Vasileiadis S, Karpouzas DG, Angelidaki I, Kotsopoulos TA. Effects of organic loading rate and hydraulic retention time on bioaugmentation performance to tackle ammonia inhibition in anaerobic digestion. Bioresource Technology. 2021;334:125246.
[7] Nam JY, Kim HW, Shin HS. Ammonia inhibition of electricity generation in single-chambered microbial fuel cells. Journal of Power Sources. 2010;195(19):6428-33.
[8] Li WW, Yu HQ, He Z. Towards sustainable wastewater treatment by using microbial fuel cells-centered technologies. Energy & Environmental Science. 2014;7(3):911-24.
[9] Rajagopal R, Massé DI, Singh G. A critical review on inhibition of anaerobic digestion process by excess ammonia. Bioresource Technology. 2013;143(17):632-41.
[10] Yenigün O, Demirel B. Ammonia inhibition in anaerobic digestion: A review. Process Biochemistry. 2013;48(5-6):901-11.
[11] De Baere LA, Devocht M, Assche PV, Verstraete W. Influence of high NaCl and NH4Cl salt levels on methanogenic associations. Water Research. 1984;18(5):543-8.
[12] Calli B, Mertoglu B, Inanc B, Yenigun O. Effects of high free ammonia concentrations on the performances of anaerobic bioreactors. Process Biochemistry. 2005;40(3):1285-92.
[13] Sprott GD, Shaw KM, Jarrell KF. Ammonia/potassium exchange in methanogenic bacteria. Journal of Biological Chemistry. 1984;259(20):12602-8.
[14] Kadam PC, Boone DR. Influence of pH on Ammonia Accumulation and Toxicity in Halophilic, Methylotrophic Methanogens. Applied and environmental microbiology. 1996;62(12):4486-92.
[15] Nam JY, Kim HW, Lim KH, Shin HS. Effects of organic loading rates on the continuous electricity generation from fermented wastewater using a single-chamber microbial fuel cell. Bioresource Technology. 2010;101(1, Supplement):S33-S7.

[16] Yang Z, Sun H, Zhou L, Arhin SG, Papadakis VG, Goula MA, et al. Bioaugmentation with well-constructed consortia can effectively alleviate ammonia inhibition of practical manure anaerobic digestion. Water Research. 2022;215:118244.

[17] Wang W, Ren X, Yang K, Hu Z, Yuan S. Inhibition of ammonia on anaerobic digestion of synthetic coal gasification wastewater and recovery using struvite precipitation. Journal of Hazardous Materials. 2017;340:152-9.

[18] Meng XS, Sui QW, Liu JB, Yu DW, Wang YW, W YS. Relieving ammonia inhibition by zero-valent iron (ZVI) dosing to enhance methanogenesis in the high solid anaerobic digestion of swine manure. Waste Management. 2020;118:452-62.

[19] Sun H, Yang Z, Zhou L, Papadakis VG, Goula MA, Liu G, et al. Calcium ion can alleviate ammonia inhibition on anaerobic digestion via balanced-strengthening dehydrogenases and reinforcing protein-binding structure: Model evaluation and microbial characterization. Bioresource Technology. 2022;354:127165.

[20] Jiang Y, McAdam E, Zhang Y, Heaven S, Banks C, Longhurst P. Ammonia inhibition and toxicity in anaerobic digestion: A critical review. Journal of Water Process Engineering. 2019;32:100899.

[21] Fan Y, Yang X, Lei Z, Zhang Z, Kobayashi M, Adachi Y, et al. Alleviation of ammonia inhibition via nano-bubble water supplementation during anaerobic digestion of ammonia-rich swine manure: Buffering capacity promotion and methane production enhancement. Bioresource Technology. 2021;333:125131.

[22] Yang Z, Sun H, Kurbonova M, Zhou L, Arhin SG, Papadakis VG, et al. Simultaneous supplementation of magnetite and polyurethane foam carrier can reach a Pareto-optimal point to alleviate ammonia inhibition during anaerobic digestion. Renewable Energy. 2022;189:104-16.

[23] Kim HW, Nam JY, Shin HS. Ammonia inhibition and microbial adaptation in continuous single-chamber microbial fuel cells. Journal of Power Sources. 2011;196(15):6210-3.

[24] Zhang JN, Zhao QL, You SJ, Jiang JQ, Ren NQ. Continuous electricity production from leachate in a novel upflow air-cathode membrane-free microbial fuel cell. Water science and technology: A journal of the International Association on Water Pollution Research. 2008;57(7):1017-21.

[25] Kim JR, Zuo Y, Regan JM, Logan BE. Analysis of ammonia loss mechanisms in microbial fuel cells treating animal wastewater. Biotechnology and Bioengineering. 2008;99(5):1120-7.

[26] Tice RC, Kim Y. Influence of substrate concentration and feed frequency on ammonia inhibition in microbial fuel cells. Journal of Power Sources. 2014;271(dec.20):360-5.

[27] Kuntke P, Geleji M, Bruning H, Zeeman G, Hamelers HVM, Buisman CJN. Effects of ammonium concentration and charge exchange on ammonium recovery from high strength wastewater using a microbial fuel cell. Bioresource Technology. 2010;102(6):4376-82.

[28] Zhao C, Wei D, Fan D, Meng S, Bian S, Zhang X, et al. Coupling of nitrifying granular sludge into microbial fuel cell system for wastewater treatment: System performance, electricity production and microbial community shift. Bioresource Technology. 2021;326:124741.

[29] Yang N, Liu H, Zhan GQ, Li DP. Sustainable ammonia-contaminated wastewater treatment in heterotrophic nitrifying/denitrifying microbial fuel cell. Journal of Cleaner Production. 2020;245:118923.

[30] Wang H, Qu Y, Li D, Zhou X, Feng Y. Evaluation of an integrated continuous stirred microbial electrochemical reactor: Wastewater treatment, energy recovery and microbial community. Bioresource Technology. 2015;195:89-95.

[31] Feng Y, Yang Q, Wang X, Logan BE. Treatment of carbon fiber brush anodes for improving power generation in air–cathode microbial fuel cells. Journal of Power Sources. 2009;195(7):1841-4.

[32] Dong H, Yu H, Wang X, Zhou Q, Feng J. A novel structure of scalable air-cathode without Nafion and Pt by rolling activated carbon and PTFE as catalyst layer in microbial fuel cells. Water Research. 2012;46(17):5777-87.

[33] Angelidaki I, Sanders W. Assessment of the anaerobic biodegradability of macropollutants. Reviews in Environmental Science and Bio/Technology. 2004;3:117-29.

[34] Ahn Y, Logan BE. A multi-electrode continuous flow microbial fuel cell with separator electrode assembly design. Applied microbiology and biotechnology. 2012;93(5):2241-8.

[35] Karthikeyan R, Selvam A, Cheng KY, Wong JWC. Influence of ionic conductivity in bioelectricity production from saline domestic sewage sludge in microbial fuel cells. Bioresource Technology. 2016;200:845-52.